Available online at www.sciencedirect.com
SCIENCE DIRECT®
Wear 255 (2003) 629–637
WEAR
www.elsevier.com/locate/wear

Wear behaviour of SiC_p-reinforced magnesium matrix composites

C.Y.H. Lim*, S.C. Lim, M. Gupta

Department of Mechanical Engineering, National University of Singapore, 10 Kent Ridge Crescent, Singapore 119260, Singapore

Abstract

This paper investigates the wear behaviour of magnesium (Mg)-based metal–matrix composites (MMCs) reinforced with silicon carbide particulates (SiC_p) during dry sliding. Experiments were conducted using a pin-on-disc configuration against a hardened tool-steel counterface under loads of 10 and 30 N, and within a sliding velocity range of 0.2–5.0 m/s. The composites exhibit slightly superior wear resistance under the lower load, but the effects of the SiC particulate reinforcements on wear resistance are not as conclusive under the higher load. Scanning electron microscopic (SEM) examinations of the worn composites identified the following wear mechanisms: abrasion, oxidation, delamination, adhesion, thermal softening and melting. The useful range of Mg/SiC_p composites appears to be limited to loads and speeds below 30 N and 5.0 m/s, respectively. Under this sliding condition, melt wear becomes the dominant wear mechanism, causing gross deformation of the magnesium matrix at the contacting interface, thus rendering any component useless.

Keywords: Metal–matrix composites (MMCs); Magnesium composites; SiC particulate reinforcements; Wear mechanisms

1. Introduction

Metal–matrix composites (MMCs) are finding increasing application in many of today's industries. In particular, the high specific strength and stiffness of aluminium (Al)-based MMCs have recommended their use in many aerospace and automotive components [1]. Wear-resistant ceramic-reinforced Al MMCs have also been used in tribological applications such as brake rotors, piston rings and cylinder liners in automobiles [2]. However, the relentless attempt by the aerospace and automotive sectors to push performance limits invariably confronts the crucial issue of weight reduction. The lightest metallic structural material is magnesium (Mg), which has a density approximately two-thirds that of aluminium. MMCs fabricated from magnesium would provide attractive alternatives to Al MMCs in the future.

Despite the potential of Mg MMCs, their study has been relatively limited when compared to the abundance of Al MMC investigations over the last two decades. Research on the tribological properties of these materials is even scarcer. Among the earliest was a study by Alahelisten et al. [3], which examined alumina-fibre-reinforced magnesium and Mg–9Al–1Zn composites in sliding, abrasion and erosion tests. They noted that sliding wear resistance did not always improve with the incorporation of alumina fibres and there was an optimum fibre content. Two-body abrasion resistance did, however, increase with increasing amounts of fibre. In contrast, fibre addition decreased wear resistance to three-body abrasion and erosion. In a later study of the sliding wear behaviour of AZ91 Mg alloy reinforced with feldspar particles, Sharma et al. [4] found that wear rates decreased with increasing reinforcement content. A transition from mild to severe wear with increasing load was noted, but the presence of the feldspar particles was able to delay this transition. More recently, Thakur and Dhindaw [5] observed that the spatial distribution of silicon carbide particulate (SiC_p) reinforcements in a magnesium matrix influenced the tribological properties of the MMC during abrasive sliding. They reported that well-dispersed SiC_p led to better microhardness, lower coefficient of friction and higher wear resistance.

One of the factors hindering the wider adoption of Mg MMCs is the lack of comprehensive property data, thus making the qualification of these materials, especially under stringent aerospace industry standards, difficult [6]. Among Al MMCs, the majority in commercial production (and therefore usage) are those reinforced with SiC_p [7]. This group of MMCs is able to offer enhanced mechanical and tribological properties at relatively low cost [8]. A recent study has shown that Mg/SiC_p MMCs also possess improved mechanical properties [9]. This paper attempts to develop a better understanding of these MMCs by exploring the tribological characteristics of Mg–9 wt.% Al alloy reinforced with SiC_p in dry sliding against a steel counterface.

* Corresponding author. Tel.: +65-6874-8082; fax: +65-6779-1459.
E-mail address: mpelimc@nus.edu.sg (C.Y.H. Lim).

0043-1648/03/$ – see front matter © 2003 Elsevier Science B.V. All rights reserved.
doi:10.1016/S0043-1648(03)00121-2

Table 1
Properties of pin specimens used in this study [11]

Material	Elastic modulus (GPa)	0.2% YS (MPa)	UTS (MPa)	Ductility (%EL)	Macrohardness (HR15T)	Density (g/cm^3)
MgAl	47.8	228	329	5.0	71.6	1.79
MgAl/SiC_p	56.1	224	268	1.2	75.1	1.90

2. Experimental details

2.1. Materials

The matrix used in this study was an alloy of magnesium with 9 wt.% aluminium. This is similar in composition to one of the popular commercial magnesium alloys, AZ91, which contains 9.5 wt.% Al, 0.5 wt.% Zn and 0.3 wt.% Mn [10]. Silicon carbide particulates with a nominal size of 14 μm were used as the reinforcement phase, at a nominal composition of 8 vol.%. Specimens were manufactured from elemental powders via power metallurgy. The powders were blended for 4 h in a tumble mixer rotating at 45 rpm. This was followed by cold compaction of the powder mixture in a 32 mm die by a single-action press delivering a pressure of 100 bar. The green compacts were then preheated to 350 °C for 30 min, before sintering at 450° for 4 h in vacuum. Finally, the sintered compacts were extruded horizontally at 350 °C using an extrusion ratio of 20.9:1.

Microstructural examination of cross-sections from the extruded specimens revealed equiaxed grains with uniformly distributed SiC_p. Tensile tests were carried out according to the ASTM E8M-96 standard using specimens of 5 mm diameter and 25 mm gauge length. The macrohardness of polished cross-sections was determined on the Rockwell 15 T superficial scale using a 1/16 in. diameter steel ball indentor with a 15 kg major load, in accordance with the ASTM E18-92 standard. Densities were calculated, based upon Archimedes' principle, from the weights of polished specimens in air and in distilled water. These properties are tabulated in Table 1. Further details of the fabrication process and characterization studies may be found elsewhere [11].

2.2. Wear testing

Dry sliding wear tests were conducted using a pin-on-disc tester. Pin specimens of diameter 5 mm and length 15 mm were machined from the as-extruded rods. Contact surfaces were prepared by grinding against 600-grit silicon carbide paper and cleaning with alcohol. A pin-holder loaded the stationary pins vertically onto a rotating AISI-O1 tool-steel disc, which had been oil-hardened to 63 HRC.

All experiments were conducted in air with temperature and relative humidity maintained between 19–23 °C and 55–67%, respectively. Two normal loads (10 and 30 N) were applied using dead weights, while five sliding speeds (0.2, 0.5, 1, 2 and 5 m/s) were selected. For each sliding condition, a total of ten 3 min tests were carried out. Prior to each test, the disc was ground against 600-grit SiC paper for a few minutes to remove accumulated debris on the wear track, followed by cleaning with alcohol. At the end of each test, the pins were carefully cleaned with alcohol and weighed using a sensitive electronic balance with an accuracy of ±0.1 mg to determine the weight loss. On certain pins, material had been extruded from the pin surface and later re-solidified around the periphery (see Section 3.2.5). Since these extruded layers should rightly be considered as material worn, they were carefully filed off prior to weighing so as not to add falsely to the weight. All weight loss data were converted to volume loss using the measured densities. Volumetric wear rates were calculated from the volume losses through a least squares analysis. The correlation coefficient in each case was greater than 0.995, indicating excellent repeatability from run to run. The worn pins surfaces and wear debris collected were examined and analysed using scanning electron microscopy (SEM) and energy dispersive X-ray spectroscopy (EDS).

3. Results and discussion

3.1. Wear rates

The volumetric wear rates for the Mg–9Al alloy and its SiC_p-reinforced composite are plotted against sliding speed in Fig. 1. It is immediately apparent that wear rates are greater at the higher load of 30 N. At the lower load of 10 N, the addition of SiC_p reinforcement brings slight but consistent improvement to the wear resistance of the MgAl

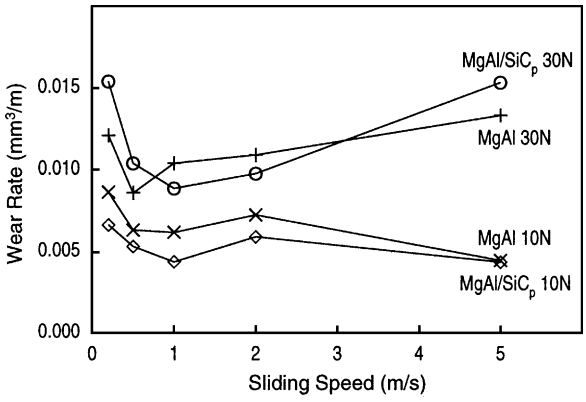

Fig. 1. Variation of wear rate with sliding speed.

Table 2
Wear mechanisms for each combination of sliding condition and pin material

Sliding speed (m/s)	Load (N)	Pin material	Wear mechanisms				
			Abrasion	Oxidation	Delamination	Adhesion	Softening/melting
0.2	10	MgAl	√√	√	√		
		MgAl/SiC_p	√√	√	√√		
	30	MgAl	√√		√√		
		MgAl/SiC_p	√√	√	√√√		
0.5	10	MgAl	√	√√	√√		
		MgAl/SiC_p	√	√√√	√		
	30	MgAl	√√		√√		
		MgAl/SiC_p	√√	√	√√√		
1	10	MgAl	√	√√	√√		
		MgAl/SiC_p	√	√√√	√		
	30	MgAl	√√		√√	√	
		MgAl/SiC_p	√√	√	√√		
2	10	MgAl	√√		√√	√	
		MgAl/SiC_p	√	√√	√		
	30	MgAl	√		√	√√	√
		MgAl/SiC_p	√		√	√√	√
5	10	MgAl	√		√	√√	√
		MgAl/SiC_p	√		√	√√	√
	30	MgAl					√√√
		MgAl/SiC_p	√				√√√

The relative extent of each wear mechanism: √: slight; √√: moderate; √√√: heavy.

alloy (about 15–30%), except at the highest speed of 5 m/s, where the wear rates are nearly equal. In contrast, under the higher load of 30 N, the presence of SiC_p appears to be marginally beneficial only at moderate speeds of 1 and 2 m/s, decreasing wear rates by 17 and 12%, respectively. Outside this speed range, SiC_p actually increases wear rates by about 15–27%.

The modest increases, and in some cases, even decreases, in wear resistance as a result of SiC_p addition are in contrast to the findings of Saravanan and Surappa [9], which showed that a 30 vol.% SiC_p Mg MMC manufactured by the melt stir technique was able to improve the wear resistance of pure magnesium by at least two orders of magnitude in pin-on-disc sliding tests at 0.5 m/s under a load range of 5–50 N. The present observations are perhaps unsurprising, since the mechanical properties of the composite, apart from the improvement in elastic modulus, are not significantly better than its monolithic counterpart.

3.2. Wear mechanisms

Scanning electron microscopic examinations of the worn pin surfaces identified five different wear mechanisms operating, either singly or in combination, under the various sliding conditions. They are: abrasion, oxidation, delamination, adhesion, and thermal softening and melting. Slight differences are noted between the type and extent of wear mechanisms operative on the Mg–Al alloy and its SiC_p composite. A detailed summary of the wear mechanisms for each combination of sliding condition and pin material is presented in Table 2. In the following sections, the observed wear mechanisms are discussed in relation to the sliding conditions and wear rates so as to better understand the tribological characteristics and identify the useful range of these MMCs.

3.2.1. Abrasion

Numerous grooves and scratch marks (Fig. 2), mostly parallel to the sliding direction, are evident on all the worn pins, except those tested under the most severe sliding condition of 30 N and 5 m/s, which are smooth and featureless (see Section 3.2.5). Grooving and scratching appear more

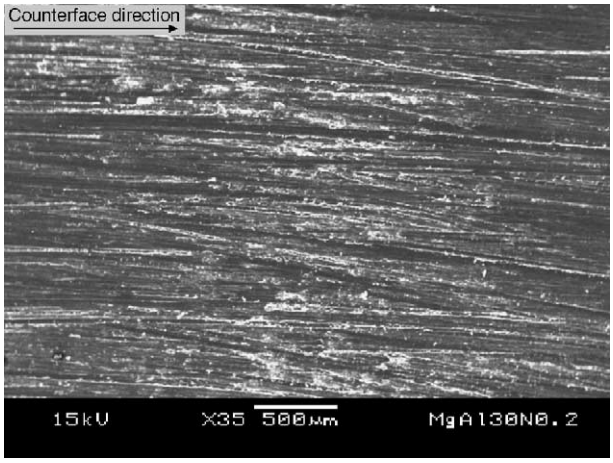

Fig. 2. Grooves and scratch marks on the pin surface indicating abrasion.

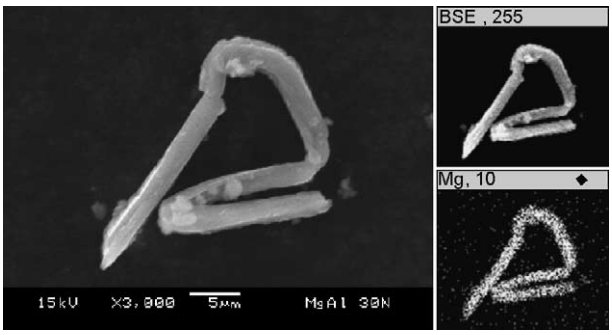

Fig. 3. Magnesium ribbon in the wear debris suggests the cutting action of an abrasive particle on the pin surface.

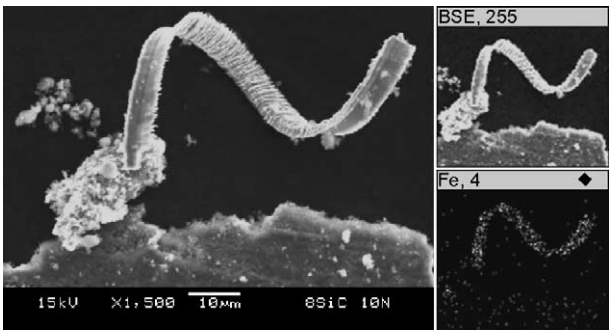

Fig. 4. Steel strip in the wear debris indicates abrasive wear of the steel counterface.

severe at the lower speeds of 1 m/s and less. Such features are characteristics of abrasion, in which hard asperities on the steel counterface, or hard particles in between the contacting surfaces, plough or cut into the pin, causing wear by the removal of small fragments or ribbon-like strips of material [12]. Fig. 3 shows a ribbon of MgAl matrix that has been lost from the pin surface through the cutting action of an abrasive particle. However, the occurrence of such ribbons in the wear debris is very rare. This suggests that abrasion took place primarily via ploughing, in which material is displaced on either side of the abrasion groove without being removed, or through wedge forming, where tiny wedge-shaped fragments are worn only during the initial contact with an abrasive particle [12].

Previous work on feldspar-reinforced AZ91 Mg composites found that abrasion was dominant under a load range of 20–40 N and speed range of 0.62–1.25 m/s [4]. In sliding tests of Al/SiC_p composites, Kwok and Lim [13] observed abrasion at low speeds between 1 and 3 m/s and loads of 10–100 N. Zhang et al. [14], testing at 0.98 m/s with stresses between 0.3 and 3 MPa, also reported severe abrasion in Al MMCs. However, this occurred only during the initial run-in period of about 50 m, after which, other mechanisms became dominant. The present observations that abrasion is dominant under lower speeds agree with the findings of these earlier studies.

It has been suggested that abrasion is extensive in Al/SiC_p composites due to the presence of dislodged and fractured SiC_p that become trapped in the sliding interface or embedded in the counterface, contributing to abrasive wear [13,14]. However, in the present investigation, based on the appearance of the worn surfaces, there is no discernible difference between the extent of abrasion on the unreinforced alloy and its SiC_p composite under the same sliding condition. It is therefore likely that dislodgement or fracture of SiC_p is limited, and abrasion is caused mainly by hard asperities on the steel disc or by work-hardened fragments of matrix alloy and steel.

Examination of the wear debris reveals the occasional presence of thin steel strips (Fig. 4), which indicates abrasion of the tool-steel counterface. Although the steel strips are associated mostly with composite pins, they are also present in debris from the unreinforced MgAl alloy. In composite pins, suitably oriented hard SiC particles would have led to cutting of the counterface. In addition, fractured SiC particles trapped between the sliding surfaces would also cause abrasion of the steel disc, as would work-hardened fragments of matrix alloy and steel. The latter is likely to be responsible for the counterface wear in sliding against unreinforced MgAl pin.

3.2.2. Oxidation

Naked-eye inspection reveals that the surfaces of the pins tested under the lower load of 10 N and at the lower speeds, especially at 0.5 and 1 m/s, appear dark, while those at the higher load and higher speeds retain their metallic lustre. Under the SEM, the dark surfaces are found to be covered extensively by a thin layer of fine particles (Fig. 5). Large amounts of fine powder are also present in the wear debris (Fig. 6). Energy dispersive X-ray spectroscopy identified strong oxygen and magnesium peaks, suggesting that the wear debris consists of magnesium oxides. These characteristics are indicative of oxidative wear, in which frictional heating during sliding causes oxidation of the surface, with wear occurring through the removal of oxide fragments

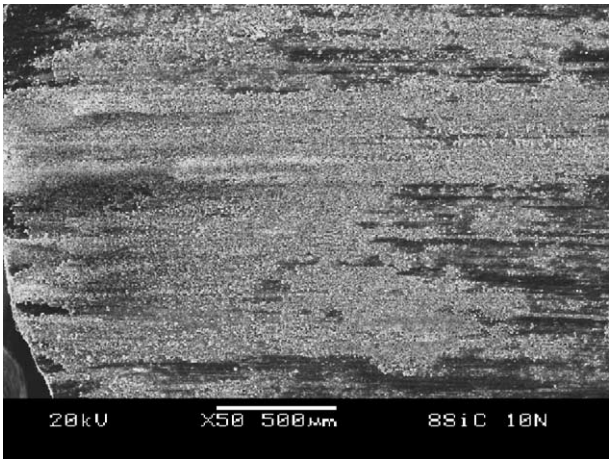

Fig. 5. Pin surface covered by a near-continuous oxide film.

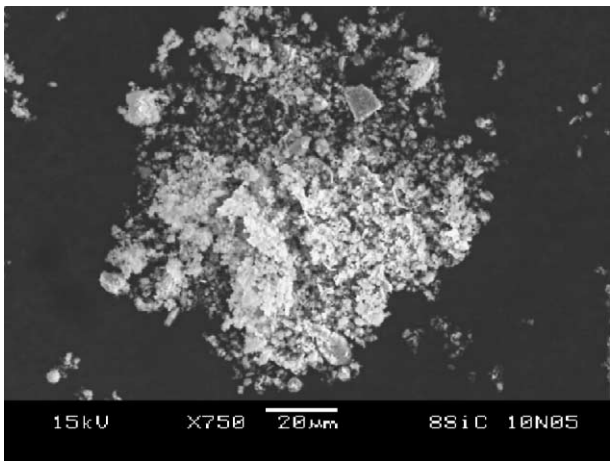

Fig. 6. Fine magnesium oxide in the wear debris.

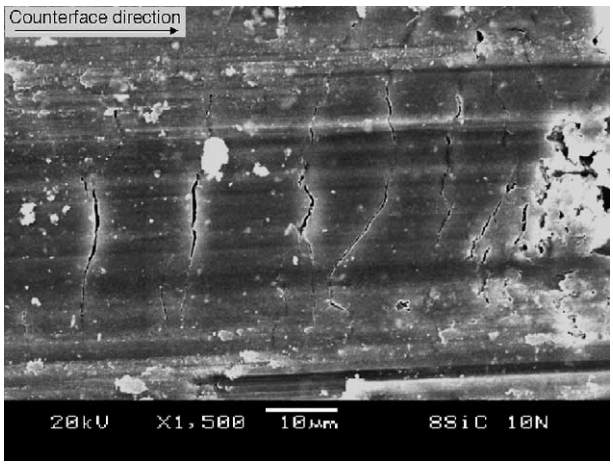

Fig. 7. Series of fine cracks perpendicular to the sliding direction on the pin surface, generally associated with delamination.

[15]. Over repeated sliding, oxide wear debris fills out the valleys on the pin surface, and becomes compacted into a protective layer; metallic contact is prevented and wear rates drop accordingly [16].

In the current study, oxide films are observed only within a certain range of sliding conditions. It has been suggested that a threshold sliding speed must be reached before asperity flash temperatures become high enough for oxidation to occur at a rate that is able to sustain a load-bearing film of adequate thickness [17]. On the other hand, there is a critical combination of load and speed, above which, the rate of removal of the oxide film through sliding becomes greater than its rate of formation, and a transition to metallic wear occurs. The point of transition is also determined by the ability of the underlying material to support the oxide film under increasing load and speed. Once the applied stresses and frictional heating become severe enough to cause plastic deformation in the bulk material, a stable protective oxide layer can no longer be maintained and metal-to-metal contact would ensue. These propositions find support in the present observation that under the 10 N load, near-continuous oxide films were found only at speeds of 0.5 and 1 m/s, while just outside this range at 0.2 and 2 m/s, the oxide film was patchy and uneven. The role of a stable oxide layer in preventing metallic wear is evident in the low wear rates recorded at 0.5 and 1 m/s. Under the higher load of 30 N, no oxide film is detected on any of the MgAl pins, while discontinuous oxide patches are observed on the composite pins at 0.5 and 1 m/s. The dominance of oxidation within this range of conditions agrees well with previous conclusions of Chen and Alpas [18], who reported that in sliding of unreinforced AZ91 Mg alloy at 0.3 m/s under loads of less than 30 N, the wear debris consisted mainly of magnesium and magnesium oxides.

Oxide films are found to be more extensive on the composites than on the unreinforced MgAl alloy, an observation shared by an earlier investigation on Al/SiC_p composites [19]. The same study also noted that the addition of SiC particles extended the mild wear regime of mixing/oxidation to higher speeds and loads. It was suggested that SiC_p reinforcements facilitate the compaction of the oxide film in between the particles [19]. Fragments of fractured SiC particles might also be mixed within the oxide layer, enhancing the hardness and wear resistance of the film [19]. Finally, the higher hardness of the composite would provide better support for the oxide film, thus improving its stability and load-bearing capacity. The benefits of SiC_p reinforcement are evident in the generally lower wear rates of the composites when oxidation is present.

3.2.3. Delamination

Pins tested at speeds of 2 m/s and less exhibit series of short cracks roughly perpendicular to the sliding direction (Fig. 7). The intersection of these cracks result in the detachment of sheet-like wear particles, leaving behind shallow craters (Fig. 8). Examination of the wear debris reveal numerous flakes or sheets (Fig. 9). In previous studies on Mg and Al alloys and their composites (see, for example

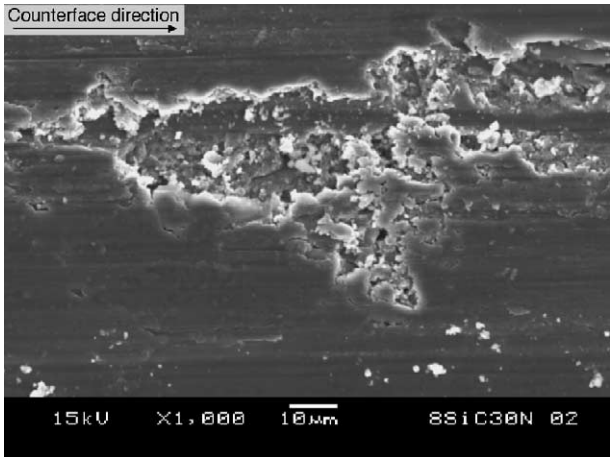

Fig. 8. Shallow crater on the pin surface where thin sheets of material have been worn away by delamination.

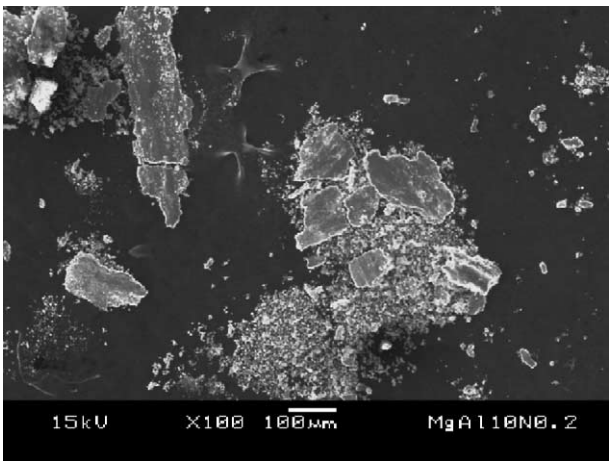

Fig. 9. Flake- or sheet-like wear debris typical of delamination.

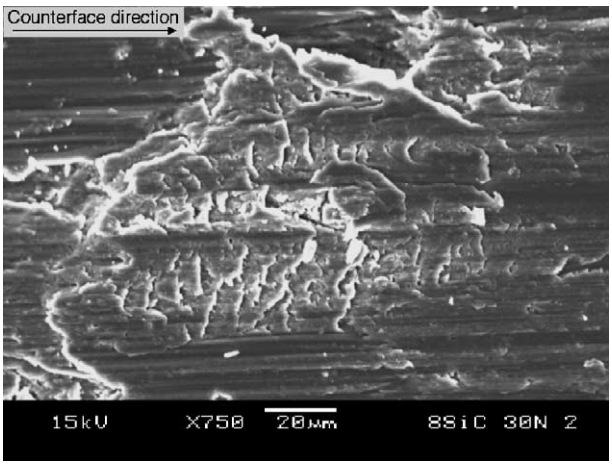

Fig. 10. Rows of furrows typical of adhesion on the pin surface.

[4,13,18,20]), such features have been linked to the process of delamination [21]. This is a fatigue-related wear mechanism in which repeated sliding induces subsurface cracks that gradually grow and eventually shear to the surface, forming long thin wear sheets [21].

Delamination is observed to more extensive under the higher load of 30 N. Earlier research has similarly found increasing dominance of delamination with load [4,18,20,22]. Since delamination involves subsurface deformation, crack nucleation and crack propagation [21], an increase in load will hasten these processes and produce greater wear. The pivotal role of crack formation and growth in delamination also accounts for the higher wear of the composites, as the SiC_p–matrix interfaces provide additional void nucleation sites, as well as preferential crack propagation paths [23]. In the present tests, wear rates for the composite are higher under the sliding conditions of 0.2 and 0.5 m/s under 30 N, where delamination is significant. This agrees with the findings of Zhang and Alpas [24], who reported that alumina (Al_2O_3) particulate reinforcements in 6061 Al alloy were not beneficial when delamination was dominant. At higher speeds of up to 2 m/s, or under the lower load of 10 N, the presence of an oxide film protected the surfaces from delamination.

3.2.4. Adhesion

At sliding speeds of 2 m/s and beyond, the features of delamination wear on are gradually replaced by rows of furrows, as shown in Fig. 10. Material transfer is evident on the pin surfaces and there are also signs of smearing and plastic deformation. Under the higher load of 30 N, the wear track on the disc is covered with a discernible layer of transferred material. The volume of wear debris is considerably less than those collected when abrasion, oxidation and delamination are dominant. The extensive transfer of material suggests that wear is of the adhesive type.

Adhesion is observed to be slightly less severe for the composite than the unreinforced alloy. This is in accordance with Archard's [25] proposal that the wear rate of a material is inversely proportional to its hardness. Comparison of the hardness data in Table 1 shows that the composite is harder than the MgAl alloy due to the addition of SiC_p, and is therefore likely to wear less. In studies of Al composites, the addition of SiC in both particulate and whisker form had also been found to lower wear rates, as well as shift the transition from delamination to adhesion to higher loads and sliding speeds [26–28].

3.2.5. Thermal softening and melting

In pins tested at 5 m/s, 10 N and 2 m/s, 30 N, layers of material are seen protruding slightly at the trailing edge. Large, irregular lumps, quite distinct from the debris morphologies hitherto discussed, are also found in the wear debris (Fig. 11). Under the most severe sliding condition of 5 m/s and 30 N, gross plastic deformation of the pin surface occurs and material is extruded from the interface before

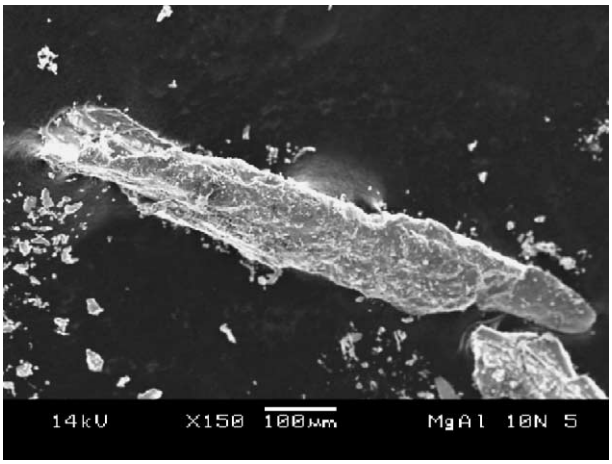

Fig. 11. Large, irregular lumps in the wear debris broken off from layers of pin material that have been deformed and extruded to the trailing edge of the pin as a result of softening and melting of the pin surface.

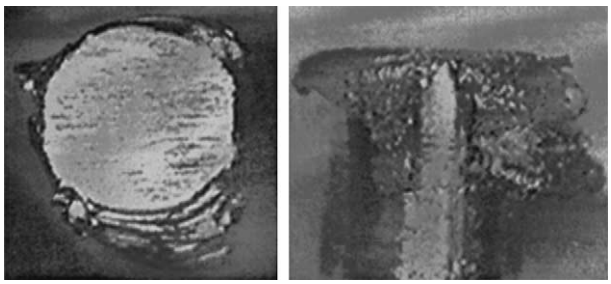

Fig. 12. Optical micrograph of the plan and side of a pin, showing extruded layers of the pin surface that have re-solidified around the periphery.

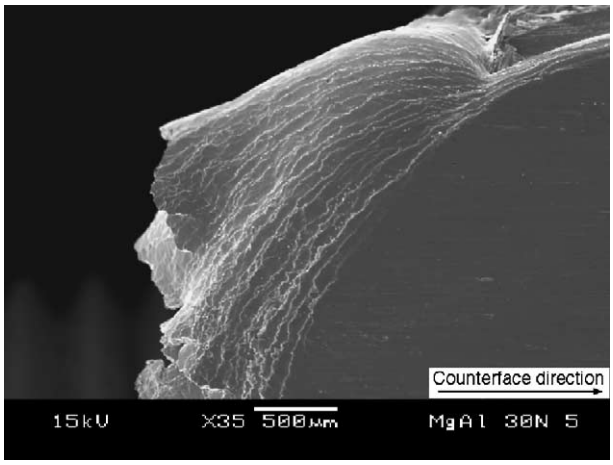

Fig. 13. SEM micrograph of the extruded layers at the trailing edge of the pin.

re-solidifying around the periphery of the pin (Figs. 12 and 13). The pin surface left behind also appears much smoother than those worn under other sliding conditions. There is extensive material transfer to the disc, which gives rise to large sheets of wear debris when it spalls (Fig. 14). A similar finding of material extrusion was earlier reported in block-on-ring sliding wear tests of AZ91 Mg alloy [18], and

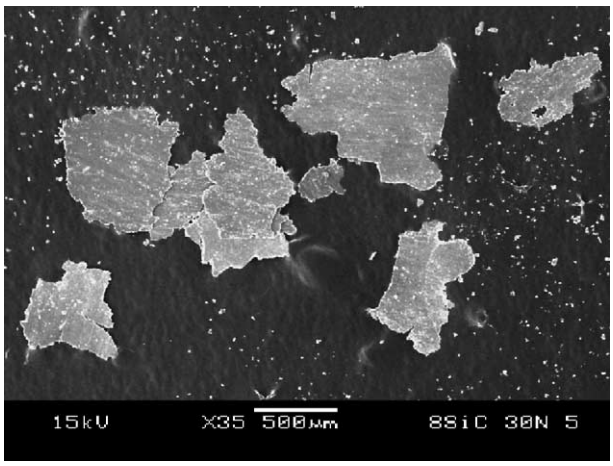

Fig. 14. Large sheets in the wear debris from the spalling of transferred pin material on the wear track.

likewise shared by previous studies of Al alloys and their composites [13,19,20]. These observations are associated with softening and melting of the matrix material caused by frictional heating at the sliding interface.

When the sliding speed and applied load reach certain critical thresholds, flash temperatures at contacting asperities could exceed the melting point of the matrix alloy, thus increasing bulk temperature and causing gradual softening of the matrix. Continued sliding or increases in speed and load would raise temperatures further, leading to melting. Previous investigations of Al composites have found the presence of SiC_p reinforcements to be beneficial in lowering wear rates and delaying the onset of these thermally activated deformation processes to higher loads and speeds [19,22,29]. This has been linked to the higher thermal stability of the composites, which allows them to retain their strengths to higher temperatures [24,27]. Contrary to these findings, the wear rates of the composite obtained in the present tests are actually higher than the unreinforced alloy. The reasons for this have yet to be determined.

4. Summary of wear behaviour

The various wear mechanisms and their regions of dominance as defined by load and sliding speed may better understood when summarized in the diagram shown in Fig. 15. In the present tests, transitions from one group of mechanisms to another are found to be gradual and the boundaries on the diagram are only approximate. Comparing Fig. 15 with the wear rates given in Fig. 1, the wear behaviour of Mg9Al alloy and its SiC_p-reinforced composites may be summarized as follows. At lower sliding speeds, delamination and abrasion are the dominant wear mechanisms. However, under the lower load of 10 N, the effects of these are mitigated by the presence of an oxide film, especially on the composites. The formation of a stable, protective oxide layer is dependent on reaching the necessary temperature at a critical sliding speed, which, in these tests, is 0.5 m/s. Under the higher load of

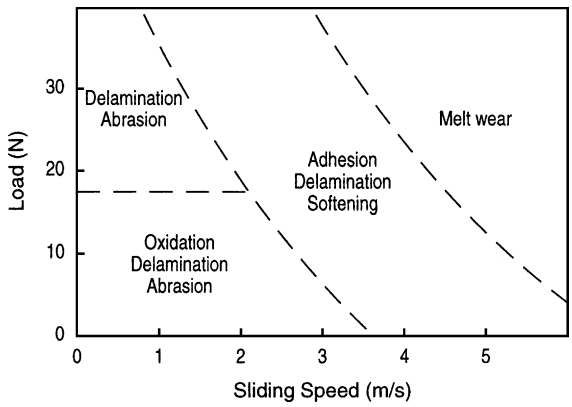

Fig. 15. Diagram illustrating the conditions and approximate boundaries of dominance of the five wear mechanisms identified in the present study.

30 N, the rate of removal of the oxide film exceeds that of its formation, and a transition from oxidation to delamination and abrasion occurs. With the dominance of delamination, the wear rates of the composites are generally higher than the unreinforced alloy because the particulate–matrix interfaces facilitate crack nucleation and growth. The increase of sliding speed above 2 m/s brings about a gradual transition from delamination to adhesion under both loads. The higher hardness of the composites improves their load-bearing capacity and imparts better resistance to adhesive wear. Further increases in speed give rise to greater frictional heating and the onset of thermally activated processes. The occurrence of softening and melting gives rise to gross plastic deformation of the pin surface, which marks the useful limit of these materials. The particulate reinforcements do not appear to be beneficial under these conditions.

5. Conclusions

1. Pin-on-disc dry sliding wear tests of Mg9Al alloy and its 8 vol.% SiC_p-reinforced composite pins against a steel counterface were carried out under loads of 10 and 30 N, and over a range of sliding speeds from 0.2–5 m/s. Five different wear mechanisms were found to operate under these conditions. They are: abrasion, oxidation, delamination, adhesion, thermal softening and melting.
2. The dominant wear mechanism under the lower load of 10 N is oxidation. The composite generally exhibits better wear resistance (15–30% improvement) due to its superior load-bearing capacity and its ability to maintain a stable oxide film, which protects against metal-to-metal contact with the steel counterface during sliding.
3. A transition from oxidation to delamination and abrasion occurs with an increase in applied load to 30 N. The wear resistance of the composite deteriorates as the presence of a second phase promotes delamination wear.
4. A gradual transition from delamination and abrasion to adhesion takes place with a rise in sliding speed under the higher load. The composite once again shows slightly improved wear resistance due to its higher load-bearing capacity.
5. At even higher speeds, increased frictional heating leads softening and melting. The massive plastic deformation experienced by the pin under 30 N and 5 m/s limits the use of the MgAl alloy and its composite to milder sliding conditions. The presence of SiC_p does not appear to be beneficial in reducing wear rates or delaying such thermally activated processes.

Acknowledgements

The authors would like to thank their colleague, Associate Professor L. Lu for many useful discussions on the fabrication and mechanical properties of MMCs. The authors also thank Mr. Yeong Wai Meng for the preparation and characterization of the pin materials. The invaluable contribution of Ms. Joycelyn Chng Siew Miang, Ms. Soh Hwee Hoon and Mr. Derrick Ang in the wear testing and analysis of the specimens is gratefully acknowledged.

References

[1] W.C. Harrington Jr., Metal matrix composite applications, in: S. Ochiai (Ed.), Mechanical Properties of Metallic Composites, Marcel-Dekker, New York, 1994, pp. 759–773.
[2] P. Rohatgi, Cast aluminium–matrix composites for automotive applications, JOM 43 (1991) 10–15.
[3] A. Alahelisten, F. Bergman, M. Olsson, S. Hogmark, On the wear of aluminium and magnesium metal matrix composites, Wear 165 (1993) 221–226.
[4] S.C. Sharma, B. Anand, M. Krishna, Evaluation of sliding wear behaviour of feldspar particle-reinforced magnesium alloy composites, Wear 241 (2000) 33–40.
[5] S.K. Thakur, B.K. Dhindaw, The influence of interfacial characteristics between SiC_p and Mg/Al metal matrix on wear, coefficient of friction and microhardness, Wear 247 (2001) 191–201.
[6] J.M. Kunze, C.C. Bampton, Challenges to developing and producing MMCs for space applications, JOM 53 (4) (2001) 22–25.
[7] M.N. Rittner, Expanding world markets for MMCs, JOM 52 (11) (2000) 43.
[8] V.K. Lindroos, M.J. Talvitie, Recent advances in metal matrix composites, J. Mater. Process. Technol. 53 (1995) 273–284.
[9] R.A. Saravanan, M.K. Surappa, Fabrication and characterisation of pure magnesium–30 vol.% SiC_p particle composite, Mater. Sci. Eng. A276 (2000) 108–116.
[10] I.J. Polmear, Light Alloys: Metallurgy of the Light Metals, third ed., Arnold, London, 1995, p. 200.
[11] W.M. Yeong, Influence of Types of Reinforcements on Properties of Magnesium Alloy, B.Eng. Thesis, National University of Singapore, 2000.
[12] K. Hokkirigawa, K. Kato, Tribol. Int. 21 (1988) 151–157.
[13] J.K.M. Kwok, S.C. Lim, High-speed tribological properties of some Al/SiC_p composites. II. Wear mechanisms, Composites Sci. Technol. 59 (1999) 65–75.
[14] Z.F. Zhang, L.C. Zhang, Y.W. Mai, Wear of ceramic particle-reinforced metal–matrix composites. Part I. Wear mechanisms, J. Mater. Sci. 30 (1995) 1961–1966.
[15] T.J.F. Quinn, The role of oxidation in the mild wear of steel, Br. J. Appl. Phys. 13 (1962) 33–37.
[16] F.H. Stott, G.C. Wood, The influence of oxides on the friction and wear of alloys, Tribol. Int. 11 (1978) 211–218.
[17] S.C. Lim, M.F. Ashby, Wear mechanism maps, Acta Metall. 35 (1987) 1–24.
[18] H. Chen, A.T. Alpas, Sliding wear map for the magnesium alloy Mg–9Al–0.9Zn (AZ91), Wear 246 (2000) 106–116.
[19] S. Wilson, A.T. Alpas, Wear mechanism maps for metal matrix composites, Wear 212 (1997) 41–49.
[20] J. Zhang, A.T. Alpas, Transition between mild and severe wear in aluminium alloys, Acta Mater. 45 (1997) 513–528.
[21] N.P. Suh, Overview of the delamination theory of wear, Wear 44 (1977) 1–16.
[22] A.T. Alpas, J. Zhang, Effect of SiC particulate reinforcement on the dry sliding wear of aluminium–silicon alloys (A356), Wear 155 (1992) 83–104.
[23] J. Zhang, A.T. Alpas, Delamination wear in ductile materials containing second phase particles, Mater. Sci. Eng. A160 (1993) 25–35.

[24] J. Zhang, A.T. Alpas, Wear regimes and transitions in Al_2O_3 particulate-reinforced aluminum alloys, Mater. Sci. Eng. A161 (1993) 273–284.
[25] J.F. Archard, Contact and rubbing of flat surfaces, J. Appl. Phys. 24 (1953) 981–988.
[26] L. Cao, Y. Wang, C.K. Yao, The wear properties of an SiC-whisker-reinforced aluminium composite, Wear 140 (1990) 273–277.
[27] A. Wang, H.J. Rack, Transition wear behavior of SiC-particulate- and SiC-whisker-reinforced 7091 Al metal matrix composites, Mater. Sci. Eng. A147 (1991) 211–224.
[28] B. Venkataraman, G. Sundararajan, The sliding wear behaviour of Al-SiC particulate composites. I. Macrobehaviour, Acta Mater. 44 (1996) 451–460.
[29] B.N. Pramila Bai, B.S. Ramasesh, M.K. Surappa, Dry sliding wear of A356–Al–SiC_p composites, Wear 157 (1992) 295–304.